Theor Chem Acc (2016) 135:203
DOI 10.1007/s00214-016-1962-1

REGULAR ARTICLE

On the choice electronic structure method to calculate the quartic potential energy surface for the vibrational calculation of polyatomic molecules

Subrata Banik[1]

Received: 12 September 2015 / Accepted: 22 July 2016 / Published online: 3 August 2016

Abstract A systematic study is made on the effects of electronic structure calculations on anharmonic spectra of polyatomic molecules. Our study is focused on the choice of electronic structure method and basis set to calculate the quartic potential energy surface (PES). We used two correlated methods Møller–Plesset perturbation theory and density functional theory with B3LYP functional and two different types of basis sets, aug-cc-pVTZ and 6-311G(2*d*,2*p*) to calculate the PES and linear DMS. For the vibrational description, we used the vibrational self-consistent field theory and the vibrational coupled cluster theory in bosonic representation.

Keywords Vibrational coupled cluster method · VSCF · Anharmonic spectra

1 Introduction

Over the years, there have been continuous efforts made for the accurate description of anharmonic vibration of polyatomic molecules. Accurate description of molecular anharmonic vibration is a computationally challenging task. One needs extensive electronic structure calculations to compute the potential energy function for the vibrational motion and an accurate ab initio method to solve the Schrödinger equation for molecular vibrations. The most commonly used form of the potential energy function is the quartic polynomial of the Taylor series expansion in the mass weighted normal coordinates

$$V(q) = \frac{1}{2}\sum_i \omega_i^2 q_i^2 + \sum_{i\le j\le k} f_{ijk} q_i q_j q_k + \sum_{i\le j\le k\le l} f_{ijkl} q_i q_j q_k q_l. \quad (1)$$

Here, q_i's are the normal coordinates and f_{ijk},f_{ijkl} are the third and fourth derivatives of electronic energy with respect to the normal coordinates at the equilibrium geometry of molecule.

The vibrational Hamiltonian with the quartic potential in Eq. 1 is a many body Hamiltonian. Consequently, the analytical solution of the corresponding Schrödinger equation is not possible. There have been extensive studies on the development of ab initio quantum chemical methods to describe molecular vibrations with such Hamiltonian [1–30]. Among these methods, the vibrational self-consistent field method (VSCF) [1–10] uses separable ansatz to calculate the vibrational energies. It can be used to calculate the vibrational spectra of large molecules and implemented in quantum chemistry program suites GAMESS and MOLPRO. Gerber and co-workers [5, 11] used a second-order perturbative correction to improve the accuracy in the VSCF calculations. To introduce the correlation effects, several ab initio methods have been developed and used by many authors [12–30]. Among these correlation methods, the vibrational coupled cluster method (VCCM) [19–26] is found to be one of the most accurate methods to describe the vibrational spectra. Recently, we made a systematic study on the implementation of VCCM method in bosonic representation [21, 22]. We found that the resultant frequencies with VCCM in bosonic representation are comparable with the full vibrational configuration interaction (FVCI) results.

✉ Subrata Banik
subratachem@gmail.com

[1] School of Chemistry, University of Hyderabad, Hyderabad 500046, India

Given a vibrational structure method, within the limitations of the approximations involved in it, the accuracy and the computational cost of the vibrational calculations depend on the electronic structure method and the basis set used for the generation of potential energy surface (PES). The use of highly accurate, e.g., coupled cluster-based method [(CCSD, CCSD(T) etc] [31, 32] with a large basis set leads to very accurate results [31–33]. However, high computational cost of these methods limits their use to small molecules. Over the past few years, several algorithms to generate such quartic PES have been developed [34–36] and some of are available as black box tools in the quantum chemistry software packages like GAUSSIAN 09, GAMESS etc. The density functional theory (DFT) and the second-order Møller–Plesset perturbation theory (MP2) are the two of the widely used electronic structure methods due to their computational efficiency and availability in all quantum chemistry software packages for medium size to large molecules. Among the DFT methods, the B3LYP is the most widely used functional. Consequently, the MP2 and B3LYP have been used extensively to generate the quartic PES for the vibrational calculations [5, 11, 18, 34, 37, 38].

Given the scenario, where accurate electronic structure methods are not feasible, there is a need to asses the reliability of the approximate but affordable methods to construct the anharmonic PESs particularly for medium size molecules. The goal of the present work is to make a comparative study on the relative accuracy of two of the methods, MP2- and B3LYP-based PES to calculate the anharmonic vibrational spectra. To pursue our purpose, we use two basis sets, correlation consistent Dunning basis set, aug-cc-pVTZ [39], and Pople basis set 6-311G(2*d*,2*p*) [40] for each of MP2 and B3LYP to generate the PES. The VSCF and VCCM in bosonic representation are used for the vibrational calculations.

The paper is organized as follows. In the next section, we give the computational details of the present study. The results are analyzed in the Sect. 3. Finally some concluding remarks are given.

2 Computational consideration

2.1 Electronic structure calculations

All the electronic structure calculations are carried out using GAUSSIAN09 program [41]. It uses the Barone algorithm [34] to generate the quartic PES in dimensionless normal coordinates. In all B3LYP calculations, the geometry optimizations were carried out tightly and the ultra-fine key word was used as recommended by Barone [34].

2.2 The vibrational self-consistent field method

The vibrational self-consistent field theory has been proposed and used extensively by many researchers [1–11] to describe anharmonic molecular vibrations in polyatomic molecules. Here, we briefly review the VSCF method. The VSCF is based on separable ansatz for the vibrational wave function. The VSCF wave function of an N mode system is written as a product of N one mode functions

$$\psi_{q_1,q_2,\ldots q_n} = \prod_i \phi^i_{n_i}(q_i). \tag{2}$$

Each of such one mode functions $\phi^i_{n_i}$ is called a modal. The modals are expanded in a basis (usually in orthogonal harmonic oscillator basis)

$$\phi^i_n = \sum_m \chi^i_m C_{mn}. \tag{3}$$

The modals are then variationally optimized by minimizing the energy with respect to these modal functions $\phi^i_n(q_i)$. The working equation for the optimized modal is

$$\left(h^{\text{scf}}_i - \epsilon^{(i)}_n\right)\phi^i_{n_i}(q_i) = 0. \tag{4}$$

The effective single particle Hamiltonian, h^{scf}_i is given by

$$h^{\text{scf}}_i = \frac{-d^2}{dq^2_i} + \sum_{n=1}^{4} u^{(n)}_i(q^n_i). \tag{5}$$

The coefficients u^n_i are the coefficients of q^n_i in the SCF potential,

$$u^{(1)}_i = \sum_{jk} f_{ijk}\langle q_j\rangle\langle q_k\rangle + \sum_j f_{ijj}\langle q^2_j\rangle + \sum_{j<k<l} f_{ijkl}\langle q_j\rangle\langle q_k\rangle\langle q_l\rangle + \sum_{j<k} f_{ijjk}\left\langle q^2_j\right\rangle\langle q_k\rangle + \sum_j f_{ijjj}\left\langle q^3_j\right\rangle, \tag{6}$$

$$u^2_i = f_{ii} + \sum_j f_{iij}\langle q_j\rangle + \sum_j f_{iijj}\langle q^2_j\rangle + \sum_{j<k} f_{iijk}\langle q_j\rangle\langle q_k\rangle, \tag{7}$$

$$u^3_i = f_{iii} + \sum_j f_{iiij}\langle q_j\rangle, \tag{8}$$

$$u^4_i = f_{iiii}. \tag{9}$$

The working equation is solved in a self-consistent manner. Starting with a set of guess basis functions, the SCF potential $u^{(n)}_i$ for a particular vibrational state is calculated. Equation 4 is then solved to obtain the modal energies and a new set of modal functions. This improved set of modal functions is then used to calculate the average SCF potential. This procedure is continued until the modal functions

are converged. The intensity of transition between vibrational ground state ψ_i^0 and excited state ψ_i^m given by

$$I_i = \frac{8\pi^2 N_A}{3hc} \nu_i |\langle \psi_i^0 | D_i^\alpha(q_i) | \psi_i^m \rangle|^2. \tag{10}$$

Here, N_A is the Avogadro's number, h is the Planck's constant, c is the speed of light and ν_i is the anharmonic transition energy for the ith state. Here, D_i^α are the expansion coefficients of the DMS along $\alpha = X, Y, Z$ direction. Note that, ψ_i^0 and ψ_i^m are not orthogonal since they are eigenfunctions of different optimized Hamiltonians. However, as pointed by Pele et al. [8], the overlap between such two VSCF wave functions is very small.

2.3 Coupled cluster method in bosonic representation

Over the last decade, there have been extensive works [19–23, 25, 26, 28] done on the formulation of vibrational coupled cluster method (VCCM) to describe molecular vibrations. Prasad and co-workers [19–23] proposed VCCM methodology in bosonic representation. Such method shows promising results for polyatomic semi-rigid molecules. Here, we summarize the VCCM in bosonic representation. The details of the method can be found in reference [19–23].

In VCCM, the wave function for vibrational ground state is parametrized as,

$$|\Psi_g\rangle = e^S e^{-\sigma} |\Phi_0\rangle. \tag{11}$$

Here, Φ_0 is the reference wave function for the ground state. A multi-dimensional Gaussian ansatz is used for this purpose. The cluster operator S and σ are consisting of connected singles, doubles, triples, etc excitation (de-excitation) operators. These cluster operators are written in terms of harmonic oscillator ladder operators a and $a^\dagger$.

$$\begin{aligned} S &= \sum_i s_i a_i^\dagger + \sum_{i \le j} s_{ij} a_i^\dagger a_j^\dagger + \sum_{i \le j \le k} s_{ijk} a_i^\dagger a_j^\dagger a_k^\dagger + \cdots \\ \sigma &= \sum_i \sigma_i a_i + \sum_{i \le j} \sigma_{ij} a_i a_j + \sum_{i \le j \le k} \sigma_{ijk} a_i a_j a_k + \cdots \end{aligned} \tag{12}$$

The working equations for the cluster operators S and σ and the ground state energy are given by

$$\langle \Phi_e | H_{\text{eff}} | \Phi_0 \rangle = 0, \tag{13}$$

$$\langle \Phi_0 | H_{\text{eff}} | \Phi_e \rangle = 0, \tag{14}$$

$$\langle \Phi_0 | H_{\text{eff}} | \Phi_0 \rangle = E_g. \tag{15}$$

Here, Φ_e are excited states, and H_{eff} is the effective Hamiltonian defined as

$$H_{\text{eff}} = e^\sigma e^{-S} H e^S e^{-\sigma}. \tag{16}$$

The excited states are then parametrized by a linear excitation operator acted on the ground state wave function

$$\Psi_e = \Omega_k e^S e^{-\sigma} |\Phi_0\rangle. \tag{17}$$

Here,

$$\Omega_k = \sum_i \Omega_i^k a_i^\dagger + \sum_{i \le j} \Omega_{ij}^k a_i^\dagger a_j^\dagger + \sum_{i \le j \le k} \Omega_{ijk}^k a_i^\dagger a_j^\dagger a_k^\dagger + \cdots \tag{18}$$

The working equation for the excitation energies is given by

$$[H_{\text{eff}}, \Omega_k] = \Delta E_k \Omega_k. \tag{19}$$

This is a vibrational CI-like equation that diagonalizes a similarity transformed Hamiltonian in the configuration space defined by the linear excitation operator Ω_k to obtain the vibrational excitation energies as eigenvalues.

Note that in the conventional coupled cluster method, the ground state wave function in Eq. 11 is parametrized with only excitation operator S.

$$\left| \Psi_g^N \right\rangle = e^S |\Phi_0\rangle. \tag{20}$$

The excited states are then obtained by diagonalization of similarity transformed Hamiltonian

$$H_{\text{eff}}^N = e^{-S} H e^S, \tag{21}$$

in the configuration manifold defined by the approximation in the excitation operator Ω.

In this study, we used the extended coupled cluster ansatz for the vibrational ground state. Such an ansatz was first proposed by Arponen [42–44]. According to the Lie algebraic decoupling theorems, the equation of motion for S is decoupled from the equation of motion of σ cluster operators [45]. We first solve the equation for S matrix elements (Eq. 13), and then using the S matrix elements, the equations for the σ matrix elements (Eq. 14) are solved. Although the use of de-excitation operator σ has no effect for the ground energy, it offers few advantages. Like the ground state ket vector, now the bra vector is also exponentially parametrized. Such exponential parametrization of ground state bra vector gives a better description of expectation values and transition matrix elements [22]. Note that the similarity transformed Hamiltonian H_{eff}^N for the excited state description is manifestly non-hermitian. Diagonalization of such non-hermitian effective Hamiltonian, depending on the truncations made may generate complex eigenvalues [46]. In the extended coupled cluster approach, we use a second similarity transformation for the effective Hamiltonian (Eq. 16). The second similarity transformation reduces the non-hermicity of the effective Hamiltonian through the first order in a nonperturbative way. Such reduction of non-hermicity of the effective Hamiltonian

Table 1 Frequencies (cm^{-1}) of vibrational fundamental transitions of F_2CO molecule

	MP2-based PES				B3LYP-based PES				
State	VSCF aug-cc-pVTZ	VSCF 6-311G(2*d*,2*p*)	VCCM aug-cc-pVTZ	VCCM 6-311G(2*d*,2*p*)	VSCF aug-cc-pVTZ	VSCF 6-311G(2*d*,2*p*)	VCCM aug-cc-pVTZ	VCCM 6-311G(2*d*,2*p*)	Exp[a]
1_1	1926.2	1940.3	1928.0	1938.7	1931.2	1948.0	1930.2	1946.0	1928
2_1	962.2	958.5	954.8	951.6	956.5	957.9	948.9	950.8	965
3_1	577.9	581.8	577.6	581.5	570.7	572.3	570.4	571.9	584
4_1	772.6	777.1	772.2	776.7	768.0	770.2	767.5	769.7	774
5_1	1226.5	1236.2	1220.1	1230.2	1198.0	1218.0	1191.6	1211.8	1249
6_1	612.9	619.9	612.0	618.9	611.5	613.1	610.5	612.1	626
SD	12	9	15	12	25	19	28	21	–

SD standard deviation

[a] Reference [48]

gives better description of the excited states as it removes some of the complex eigenvalues [21].

Once the effective Hamiltonian Eq. 16 is diagonalized, the square of the dipole transition matrix elements are obtained by effective operator approach [47]. The working equations for the intensity of a vibrational transition are given by

$$\begin{aligned} I_i &= \frac{8\pi^2 N_A}{3hc}\Delta E_f \left|\left\langle \Psi_i \left| D^{\alpha}_{\text{eff}} \right| \Psi_f \right\rangle\right|^2 \\ &= \frac{8\pi^2 N_A}{3hc}\Delta E_f \left\langle L_i \left| D^{\alpha}_{\text{eff}} \right| R_f \right\rangle \left\langle R_f \left| D^{\alpha}_{\text{eff}} \right| L_f \right\rangle, \end{aligned} \tag{22}$$

where ΔE_f is the transition energy, L_i and R_i are the left and right eigenvectors of H_{eff} and the effective dipole operator D^{α}_{eff} is given by

$$D^{\alpha}_{\text{eff}} = e^{\sigma} e^{-S} D^{\alpha} e^{S} e^{-\sigma}. \tag{23}$$

In all VCCM calculations, we used four boson operators for the ground state cluster matrix elements S and σ and for the excitation operator Ω.

2.4 Approximation for dipole moment surface

The calculations of the transition intensity using Eqs. 10 or 22 require the similar Taylor series expansion of electronic dipole surface (DMS) as in case of the PES generation. A cubic polynomial in the Taylor series expansion

$$D^{\alpha}(Q) = d^{\alpha}_{e} + \sum_{i} d^{\alpha}_{i} Q_i + \sum_{i,j} d^{\alpha}_{ij} Q_i Q_j + \sum_{i,j,k} d^{\alpha}_{ijk} Q_i Q_j Q_k. \tag{24}$$

is usually used when a quartic PES is used for the calculations. The generation of such cubic DMS makes the calculations computationally costlier to a greater extent. In this work, we approximate the above expansion only up to linear terms. From the results of our recent study [24], we anticipate that the errors in the intensities for such approximation will be minimum for the fundamental transitions. Even though the contribution of the quadratic and cubic terms of DMS for the fundamental transition intensities are non-zero, we expect that such contribution will be very less compared to the contribution from the linear terms in the DMS for intensities of the fundamental transitions.

3 Results and discussion

3.1 F_2CO

The first molecule we studied is F_2CO. We present the fundamental transition energies in Table 1. The calculated results are compared with the available experimental values [48]. We follow the standard Mulliken convention for indexing the vibrational modes. The six normal modes span the $3A_1 + 1B_1 + 2B_2$ symmetries in F_2CO. We find good agreements between the experimental results and calculated results for the fundamental transitions. We have calculated the standard deviations with respect to the experimental values to get some quantitative comparison between the MP2 and B3LYP methods and the two different basis sets. Here, we find that the MP2-based calculations give better results than the B3LYP-based calculations for the transition energies. In case of VSCF, the standard deviation for the fundamental transition energies is about $12\,cm^{-1}$ with MP2/aug-cc-pVTZ-based PES, whereas the B3LYP/aug-cc-pVTZ-based PES gives about $25\,cm^{-1}$. Similarly, in VCCM calculations, the MP2/aug-cc-pVTZ gives standard deviation about $15\,cm^{-1}$, whereas the B3LYP/aug-cc-pVTZ gives about $28\,cm^{-1}$. Between the two basis sets, we find the 6-311G(2*d*,2*p*) provides marginally better results for the fundamental transition energies in all the calculations.

Table 2 Intensities (km/mol) of vibrational fundamental transitions of F_2CO molecule

	MP2-based PES and DMS				B3LYP-based PES and DMS				
State	VSCF aug-cc-pVTZ	VSCF 6-311G(2*d*,2*p*)	VCCM aug-cc-pVTZ	VCCM 6-311G(2*d*,2*p*)	VSCF aug-cc-pVTZ	VSCF 6-311G(2*d*,2*p*)	VCCM aug-cc-pVTZ	VCCM 6-311G(2*d*,2*p*)	Exp[a]
1_1	424.4	375.8	314.2	340.9	461.4	411.3	403.7	382.6	381.7
2_1	64.2	59.2	63.8	58.7	61.0	54.0	60.6	53.5	56.4
3_1	6.1	6.0	6.0	5.9	4.9	4.8	4.8	4.7	5.2
4_1	31.7	33.1	32.1	33.5	34.3	33.6	34.7	33.9	30.6
5_1	408.1	390.8	409.0	390.9	414.3	389.1	414.8	388.9	370.8
6_1	6.3	6.0	6.2	5.9	5.8	6.0	5.6	5.8	7.0
SD	25.6	9.5	23.8	10.2	40.7	15.7	38.5	14.2	–

SD standard deviation

[a] Reference [48]

In Table 2, we present the intensities for the fundamental transitions and compared the results with the experimental values [48]. As mentioned earlier, we used only linear dipole moment surface for our calculations. We find that between MP2- and B3LYP-based calculations, again MP2 gives better accuracy than B3LYP. The standard deviation for the VSCF calculations is 25.6 km/mol with MP2/aug-cc-pVTZ-based PES and DMS, and 40.7 km/mol with B3LYP/aug-cc-pVTZ surfaces. Again for the VSCF calculations, the standard deviation is 9.5 km/mol with MP2/6-311G(2*d*,2*p*) surfaces against 15.7 km/mol with B3LYP/6-311G(2*d*,2*p*) surfaces. The standard deviations for the VCCM results are 23.8 km/mol with MP2/aug-cc-pVTZ, 10.2 km/mol with MP2/6-311G(2*d*,2*p*), 38.5 km/mol with B3LYP/aug-cc-pVTZ and 14.2 km/mol with B3LYP/6-311G(2*d*,2*p*)-based PES and DMS. We note that since the 2_2 state is strongly coupled with the 1_1 state, the 1_1 and 2_2 transitions intensities in the VCCM calculations to be added to calculate the deviations of the 1_1 intensity compared to the experiment. Experimentally [49, 50] one gets a broad band in this frequency region (see Fig. 1).

In Fig. 1, we present the vibrational spectra of F_2CO in the range 500–3500 cm^{-1} obtained by the VCCM. Note that the accurate description of the overtones and combination bands requires higher-order DMS. However, if a two or higher quanta excited state is strongly coupled with a fundamental state, then it borrows significant intensities from the fundamental transition. The VCCM due to its VCI like structure to describe the excited states, is able to describe such vibrational coupling accurately. The VSCF, on the other hand, gives poor description of such coupling effects. Moreover, the combination states can not be obtained by VSCF method with a linear DMS. Hence, we exclude the VSCF spectra from the figure. All the four spectra obtained from quartic PES and linear DMS calculated by MP2 with aug-cc-pVTZ and 6-311G(2*d*,2*p*) basis sets and B3LYP with aug-cc-pVTZ and 6-311G(2*d*,2*p*) basis sets are compared with the experimental infrared (IR) spectrum. The experimental spectrum is taken NIST Chemistry Web Book database [49, 50]. This spectrum shows typical rotational profile of the peaks. However, in our treatment, we considered the molecule is non-rotating. The calculated spectra are in good agreement with the experimental one. The experimental spectrum shows a broad band in the region around 1500 cm^{-1}. In our calculations, we find two medium intense peak in this region corresponds to transitions to 4_2 and 2_16_1 states. The broad band near 1900 cm^{-1} includes 5_16_1 and 2_2 along with the fundamental transition 1_1. Due to strong coupling between 1_1 and 2_2 states, the 2_2 transition borrows significant intensity from the 1_1 transition. Again, there are two medium intense broad bands at around 2100 cm^{-1} and 2400 cm^{-1}. With our calculations, we assign these transitions as 2_15_1 and 5_2 transitions respectively. The calculated transitions for these transitions are less intense compared to the experimental peaks. The absence of higher-order DMS is the reason for such low intensities for these transitions in the calculated spectra. In between the spectra calculated by using MP2 surfaces and B3LYP surfaces, we found that most of the peaks appear at lower frequencies in the B3LYP spectra than the MP2 spectra. As can be noticed from Table 1, except for 1_1 transition, the B3LYP-based calculations underestimate the fundamental frequencies to a greater extent than the MP2-based calculations. Consequently, the transition energies for the overtone and combination bands are also underestimated by B3LYP method. For example, the bands correspond to 5_16_1, 2_15_1, 5_2 transitions appear at lower frequencies in B3LYP/aug-cc-pVTZ spectrum compared to MP2/aug-cc-pVTZ spectrum.

3.2 1,1-Difluoroethene (1,1-$F_2C_2H_2$)

The second example that we studied is 1,1-$F_2C_2H_2$. Over the years, the vibrational spectrum of this molecule has

Table 3 Frequencies of fundamental transitions of 1,1-$F_2C_2H_2$ molecule

MP2-based PES					B3LYP-based PES				
State	VSCF aug-cc-pVTZ	VSCF 6-311G(2*d*,2*p*)	VCCM aug-cc-pVTZ	VCCM 6-311G(2*d*,2*p*)	VSCF aug-cc-pVTZ	VSCF 6-311G(2*d*,2*p*)	VCCM aug-cc-pVTZ	VCCM 6-311G(2*d*,2*p*)	Exp[a]
1_1	3107.1	3107.0	3093.0	3058.9	3052.9	3056.5	3011.1	3016.2	3058.1
2_1	1745.3	1746.3	1731.6	1728.6	1738.9	1744.9	1724.2	1729.3	1728.5
3_1	1398.3	1412.9	1341.2	1354.1	1394.7	1396.7	1357.3	1357.5	1358.9
4_1	935.2	933.6	927.9	926.6	929.2	930.4	921.9	923.3	925.8
5_1	548.5	551.8	548.1	551.4	545.3	544.8	545.0	544.4	549.6
7_1	832.7	836.4	749.7	756.6	863.4	856.5	790.0	782.1	802.1
8_1	627.7	635.3	623.7	631.6	626.1	632.3	619.9	625.4	609.5
9_1	3179.5	3178.9	3201.5	3206.4	3105.6	3110.4	3148.5	3154.0	3175.6
10_1	1302.5	1321.7	1287.3	1306.2	272.7	1293.5	1258.5	1278.6	1301.2
11_1	970.7	975.2	935.5	940.8	962.8	964.5	929.2	930.0	953.8
12_1	455.5	460.2	426.5	431.7	456.8	456.2	429.7	427.9	436.9
SD	25	30	24	19	34	34	24	20	–

SD standard deviation

[a] Reference [57]

been subject of number of experimental [51–57] and theoretical studies [48, 57, 58]. The presence of number of strong Fermi resonances and higher quanta resonances makes it fairly complex to assign its vibrational transitions. We find some ambiguities in the spectral intensities reported in different literatures. Kagel et al. [51] and Nielsen et al. [59] reported relatively intense fundamental transitions corresponds to CH stretches. Bruns' [48, 51] results show that transition to CH asymmetric stretch fundamental appears with intensity 8.6 km/mol and symmetric stretch appears with intensity 42.2 km/mol. However, McKean et al. [57] reported two weak transitions correspond to these two CH stretches in their experiment. McKean et al. [57] also assigned some combination bands in this region (frequency range 3000–3500 cm^{-1}). All of these transitions are found to be weak. Recently, Krasnoshchekov et al. [58] used Van Vleck perturbation theory to study its vibrational spectrum. These authors used a full quartic and semi-diagonal sextic PES and a cubic DMS to describe the anharmonic effects in its spectrum. Their theoretical intensity for

Table 4 Intensities (km/mol) of vibrational fundamental transitions of 1,1-$F_2C_2H_2$ molecule

MP2-based PES and DMS					B3LYP-based PES and DMS				
State	VSCF aug-cc-pVTZ	VSCF 6-311G(2*d*,2*p*)	VCCM aug-cc-pVTZ	VCCM 6-311G(2*d*,2*p*)	VSCF aug-cc-pVTZ	VSCF 6-311G(2*d*,2*p*)	VCCM aug-cc-pVTZ	VCCM 6-311G(2*d*,2*p*)	Exp[a]
1_1	7.7	6.3	2.7	2.0	5.9	4.8	2.8	2.8	42.2
2_1	272.9	255.5	178.5	141.7	292.5	273.4	225.7	171.7	216.0
3_1	3.5	3.2	0.3	0.2	3.7	2.7	0.9	0.5	0.0
4_1	68.4	64.7	67.5	63.7	76.7	72.0	76.0	71.4	64.8
5_1	4.9	4.5	4.8	4.5	4.3	4.0	4.2	3.9	5.1
7_1	75.6	79.5	72.2	72.8	78.3	74.7	74.6	70.7	60.3
8_1	0.1	1.5	0.2	2.8	0.0	0.2	0.0	0.4	0.3
9_1	1.4	0.6	1.1	0.3	0.3	0.0	0.1	0.0	8.6
10_1	225.7	204.5	208.1	184.1	224.6	202.1	221.3	197.5	190.1
11_1	19.9	18.5	20.2	17.3	27.3	23.4	24.6	21.3	23.5
12_1	0.8	1.2	0.8	1.2	0.6	1.0	0.7	1.0	0.6
SD	24.4	16.5	15.5	28.1	31.6	22.0	15.0	17.0	–

The standard deviation calculation excludes the CH stretching fundamentals

SD standard deviation

[a] Reference [48]

the symmetric CH stretch is 2.79 km/mol and for asymmetric CH stretch is 1.08 km/mol. Moreover, the reported experimental spectrum in the NIST database [49, 50] does not show any intense peak in this region. Such ambiguities make this molecule a good subject for our study.

We present the excitation energies for transitions to the fundamental states with MP2 and B3LYP PES and linear DMS in Table 3. Following the Mulliken notations, the 12 normal modes of vibration span as $5A_1 + 1A_2 + 2B_1 + 3B_2$ symmetries. We compare the fundamental transition frequencies with the experimental gas phase frequencies [57]. Like F_2CO, here also we find good agreement between the experimental values and theoretical results. The maximum value of the standard deviation in the transition energy is only 34 cm^{-1} when VSCF method and B3LYP/aug-cc-pVTZ-based PES are used in the calculations.

In between MP2 and B3LYP, both the methods give nearly identical accuracy for the transition energies compared to experimental values in VCCM-based calculations. In case of VSCF calculations, the MP2-based PES gives more accuracy than B3LYP-based PES. For example, in VCCM calculations, the standard deviation is 24 cm^{-1} with both MP2/aug-cc-pVTZ and B3LYP/aug-cc-pVTZ surfaces. The standard deviations in the VSCF calculations are 25 and 34 cm^{-1} with MP2/aug-cc-pVTZ and B3LYP/aug-cc-pVTZ surfaces respectively. We note that the differences between MP2 results and B3LYP results are marginal except for the 1_1, 9_1, 10_1 and 11_1 states. In these four fundamental transitions (1_1, 9_1, 10_1, 11_1), we find large

Table 5 Frequencies (cm^{-1}) and intensities (km/mol) of fundamental transitions of Pyridine molecule: MP2 and B3LYP calculations with 6-311G(2*d*,2*p*) basis set

Frequency						Intensity				
State	VSCF MP2	VSCF B3LYP	VCCM MP2	VCCM B3LYP	Exp.[a]	VSCF MP2	VSCF B3LYP	VCCM MP2	VCCM B3LYP	Exp.[a]
1_1	3114.9	3062.0	3079.0	3006.3	3094	4.5	7.6	0.0	0.7	0.0
2_1	3065.0	3005.2	3076.9	3046.3	3073	5.7	5.5	0.1	0.1	1.5 ± 1.0
3_1	3068.1	2995.4	2990.4	2968.4	3030	3.7	7.3	0.0	0.0	8.5 ± 0.0
4_1	1597.0	1598.2	1574.8	1576.0	1584	13.0	22.5	9.0	19.9	17.9 ± 1.8
5_1	1490.9	1496.2	1476.6	1480.9	1483	3.6	3.4	3.9	3.5	4.0 ± 0.4
6_1	1230.9	1229.6	1218.7	1219.3	1218	1.3	3.0	1.2	1.7	4.3 ± 0.4
7_1	1084.0	1084.7	1069.4	1069.2	1072	1.8	2.2	2.3	2.9	4.5 ± 0.5
8_1	1037.1	1038.2	1030.5	1030.8	1032	9.0	8.5	8.6	7.7	7.7 ± 0.8
9_1	994.5	1001.5	988.0	995.2	991	4.8	5.3	4.7	5.5	5.5 ± 0.5
10_1	603.9	612.5	598.8	607.5	601	4.5	4.6	4.5	4.6	4.4 ± 0.4
16_1	766.3	772.1	740.9	748.5	744	8.8	5.0	2.1	1.6	12.9 ± 1.3
17_1	757.8	747.9	696.2	683.4	700	61.4	62.1	64.4	62.4	67.5 ± 6.7
18_1	415.4	421.1	403.1	408.3	403	3.5	3.4	3.6	3.2	7.2
19_1	3071.2	3009.8	3097[b]	3061.1	3094	21.1	26.9	8.9[b]	6.5	15.9 ± 1.6
20_1	3038.3	2965.4	3070.8	3010[c]	3042	18.2	27.4	8.2	18.3[c]	5.1 ± 1.5
21_1	1586.1	1593.0	1567.0	1570.7	1581	2.1	7.6	2.6	8.3	7.3 ± 1.8
22_1	1456.2	1457.2	1441.4	1440.8	1442	19.8	26.1	19.2	26.2	31.1 ± 3.1
23_1	1375.4	1372.1	1353.0	1354.5	1362	0.5	0.1	0.1	0.0	0.5 ± 0.2
24_1	1345.0	1256.9	1333.5	1224.4	1227	0.9	0.1	1.1	0.2	0.0
25_1	1171.3	1163.8	1154.1	1146.9	1143	1.3	2.4	1.1	2.4	3.6 ± 0.4
26_1	1067.8	1068.5	1045.0	1059.9	1079	0.2	0.1	0.4	0.0	0.0
27_1	658.1	665.0	654.2	661.1	654	0.3	0.2	0.4	0.2	1.1 ± 0.2
SD	24	32	24	20	–	29.9	22.8	25.3	18.5	–

[a] Reference [66]

[b,c] We found two states very close lying. The intensity value is the sum of these two. See text for details

Table 6 Medium intense overtones and combination states of Pyridine in the frequency range over 3000 cm^{-1} obtained by VCCM method using MP2-based PES and DMS

State	Frequency (cm^{-1})	Intensity (km/mol)
$9_1 10_1 17_2$	3053.3	3.3
$12_1 16_1 22_1$	3055.5	2.7
$5_1 20_1$	3036.1	1.0
$12_2 13_1 17_1$	3052.6	2.7
$11_1 12_1 13_1 17_1$	3064.2	2.5
$6_1 12_1 14_1$	3073.2	2.4
$4_1 21_1$	3142	3.3

differences in the transition energy values between the results calculated by MP2 and B3LYP PES. For example, in the VCCM calculation, B3LYP underestimates the CH symmetric stretching (1_1) frequency with both the basis sets, whereas MP2 with aug-cc-pVTZ overestimates it. The MP2 with 6-311G(2*d*, 2*p*) gives the experimental value for this transition.

In Table 4, we present the intensities for the fundamental transitions with linear DMS. The results are compared with the experimental values [48]. For this molecule, we find that the B3LYP gives better accuracy than MP2 for VCCM calculations. However, for the VSCF calculations, MP2 gives more accurate results. For example, for VCCM calculations, the standard deviations with MP2/6-311G(2*d*,2*p*) surfaces is 28 km/mol, whereas with B3LYP/6-311G(2*d*,2*p*) surfaces is 17 km/mol. In between the two basis sets used here, 6-311G(2*d*,2*p*) basis set is found to give more accurate results. Note that due to ambiguities in the reported experimental intensity values for the CH fundamentals found in the literatures, we exclude the intensities of 1_1 and 9_1 transitions in our standard deviation calculation.

A comparison between the experimental spectrum [49, 50] and our VCCM spectra is given in Fig. 2. The calculated spectra are qualitatively in good agreements with the experimental one, except for the frequency region 1200–1800 cm^{-1}. We found that the broad band with a shoulder at around 950 cm^{-1} corresponds to 4_1 and 11_1 fundamental transitions together. With MP2/6-311G(2*d*,2*p*) calculations, the 11_1 transition is visible as shoulder peak. The experimental spectrum shows a broad band around 1250 cm^{-1}. In our calculations, we found very intense 10_1 fundamental along with combination bands $6_1 8_1$, $4_1 12_1$, $6_1 7_1$ and $7_1 8_1$ in this region. These calculated combination bands near 10_1 fundamental are found to be more intense by MP2-based calculations than B3LYP-based calculations. Again, the

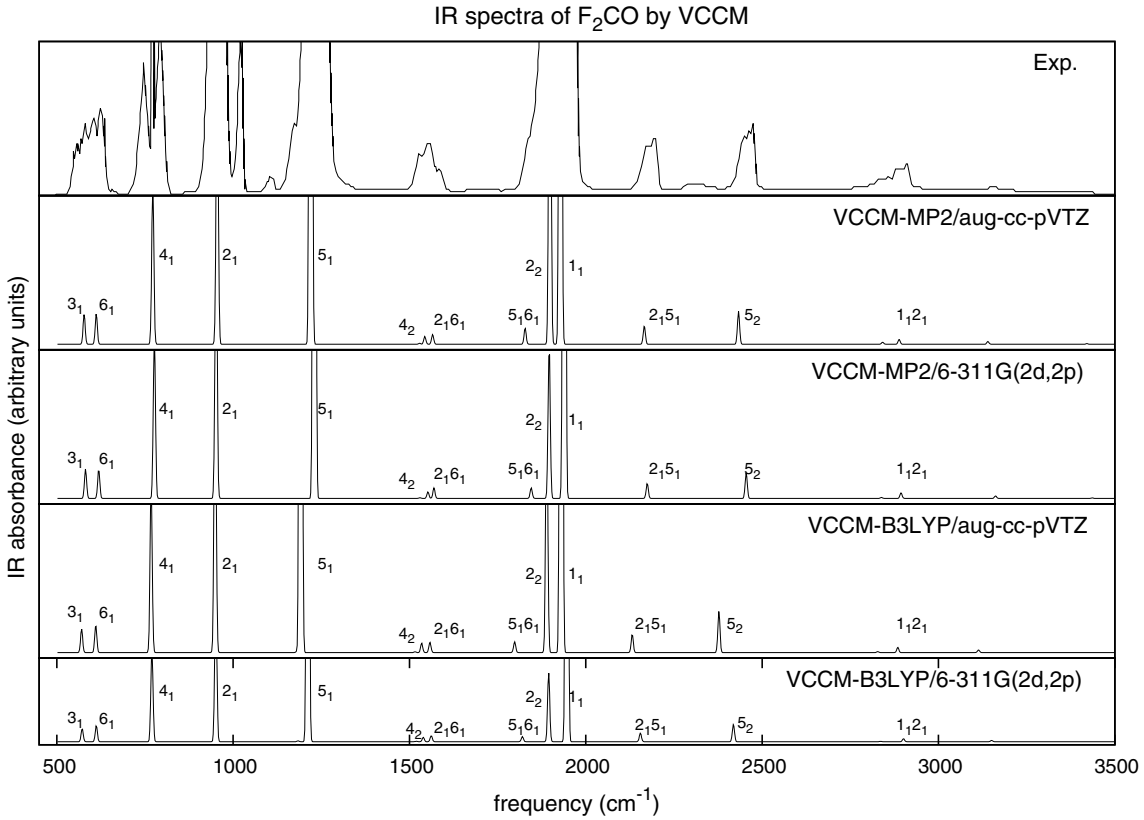

Fig. 1 Comparison of theoretical spectra of F_2CO molecule calculated by VCCM method with experimental gas phase spectrum [49]

experimental spectrum shows two broad band in 1500-1800 cm^{-1} region. In our VCCM-MP2/aug-cc-pVTZ spectrum, we found two intense close peaks around 1700 cm^{-1} and one weak intense peak near 1500 cm^{-1}. In VCCM-MP2/6-311G(2*d*,2*p*) spectrum, one relatively broad peak appears near 1700 cm^{-1} and one low intense peak appears near 1500 cm^{-1}. In both VCCM-B3LYP/aug-cc-pVTZ and VCCM-B3LYP/6-311G(2*d*,2*p*) spectra, there are one intense peak and one weak peak near 1700 cm^{-1} and one weak intense peak near 1500 cm^{-1}. We found three overtone and combination transitions in this region along with the 2_1 fundamental. Among these three, the $6_1 8_1 12_1$ and $10_1 12_1$ combination band appears near 1700 cm^{-1} and the other one 7_2 appears near 1500 cm^{-1}. The fundamental 2_1 and the combination states $6_1 8_1 12_1$ and $10_1 12_1$ together form one intense broad band with the experimental resolution. We note that the 7_2 overtone transition also observed by McKean et al. [57], but at 1611 cm^{-1} (reported as 11_2 in Table 1 in reference). Note that our convention of numbering the vibrational modes is different than the convention followed by McKean et al. [57] due to different orientation of the molecular axis. In our calculations, we find large deviations in both transition energy and intensity for this 7_2 transition. With MP2/aug-cc-pVTZ-based calculations, the 7_2 transition energy is 1484 cm^{-1}, whereas, with B3LYP/aug-cc-pVTZ-based calculation, the value is 1565 cm^{-1}. The calculated intensity value for this transition found to be very less in all our calculations compared to the experiment. The use of linear DMS is not adequate to account the high intensity value of this transition. Lastly, we assign the weak and broad band around 3000 cm^{-1} as CH stretching fundamentals 1_1 and 9_1 along with some higher quanta states that are coupled strongly with these fundamentals. Note that with B3LYP-based calculations, we get only 1_1 transition, whereas the MP2-based calculations give both 1_1 and 9_1 transitions.

3.3 Pyridine

The largest molecule in this study is pyridine. There have been several experimental studies [60–64] on the vibrational spectra of this molecule due to its chemical and biological importance. Most of the experimental results and assignments are summarized by Klots [65]. A few theoretical studies on the vibrational spectra of this molecule came to our notice [66, 67]. Recently, Partal et al. [61] made the vibrational analysis of this molecule by inelastic neutron scattering experiments and made assignment of the

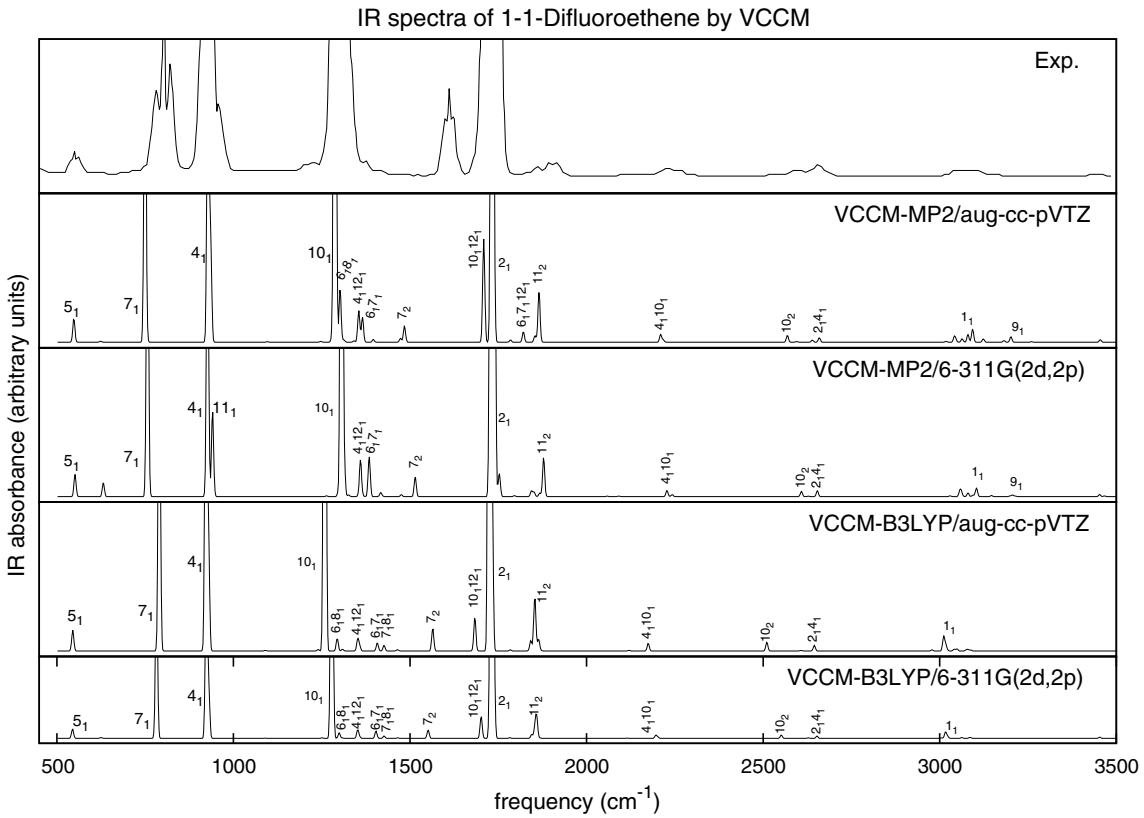

Fig. 2 Comparison of theoretical spectra of 1-1-$F_2C_2H_2$ molecule calculated by VCCM method with experimental gas phase spectrum [49]

vibrational excitation by ab initio studies. All the earlier studies pointed the complexity of the vibrational analysis of pyridine both theoretically and experimentally. The 27 normal modes of vibrations span as $10A_1 + 5A_2 + 3B_1 + 9B_2$ irreducible representations in the C_{2V} point group. Out of these, $5A_2$ modes are IR inactive. We present the comparisons of our results with the experimental results [66] in Table 5. Since in the earlier two molecules we found that the 6-311G(2*d*,2*p*) basis set gives a better description in both the VSCF- and VCCM-based calculations, we restrict ourselves only to this basis set.

For this molecule, we note that MP2 and B3LYP give nearly identical errors in the transition energies of the fundamental excitations. With the MP2 calculations, the standard deviation for the VSCF fundamental transition energies is about 24 cm^{-1}, whereas, with B3LYP, the standard deviation is 32 cm^{-1}. Again the VCCM gives the standard error about 24 cm^{-1} with MP2 PES, whereas with B3LYP the standard deviation is 20 cm^{-1}.

Turning to the intensity values, we found that the B3LYP gives more accurate results for both VSCF and VCCM calculations. The standard deviation with MP2-based surface is 25 km/mol, whereas with B3LYP the standard deviation is 18.5 km/mol in the VCCM calculations. In VSCF calculations, the standard deviation is 29.9 km/mol with MP2 and 22.8 km/mol with B3LYP surfaces.

For the CH-stretching region, i.e. the frequency range 3000–3500 cm^{-1}, we find many transitions with intensity values more than 1.0 km/mol. Due to strong resonances, the fundamental states mixes strongly with higher quanta excited states. The harmonic intensities of the 5 CH stretches get distributed over these states. In Table 6, we present the VCCM results of some of these states with MP2-based calculations. We note that the 19_1 state mixes strongly with $10_1 14_1 18_1 26_1$ combination states. This results two almost degenerate states $19_1 + 10_1 14_1 18_1 26_1$ at 3097 cm^1 and $19_1 - 10_1 14_1 18_1 26_1$ at 3098 cm^{-1} with intensity 4.7 km/mol and 4.2 km/mol, respectively. We assign these transitions together as 19_1 fundamental. Similarly in B3LYP-based calculations, the 20_1 fundamental is strongly coupled with $9_1 10_1 13_1 14_1$ and $16_1 17_1 21_1$ combination states. Here also two states are found at 3009 and 3012 cm^{-1} with intensity 8.5 km/mol and 10.5 km/mol. We assign these transitions together as 20_1 fundamental.

In Fig. 3, the VCCM spectra obtained by using MP2- and B3LYP-based surfaces are compared with the experimental gas phase spectrum [49, 50]. The experimental spectrum shows a broad band around 3000 cm^{-1} region with three

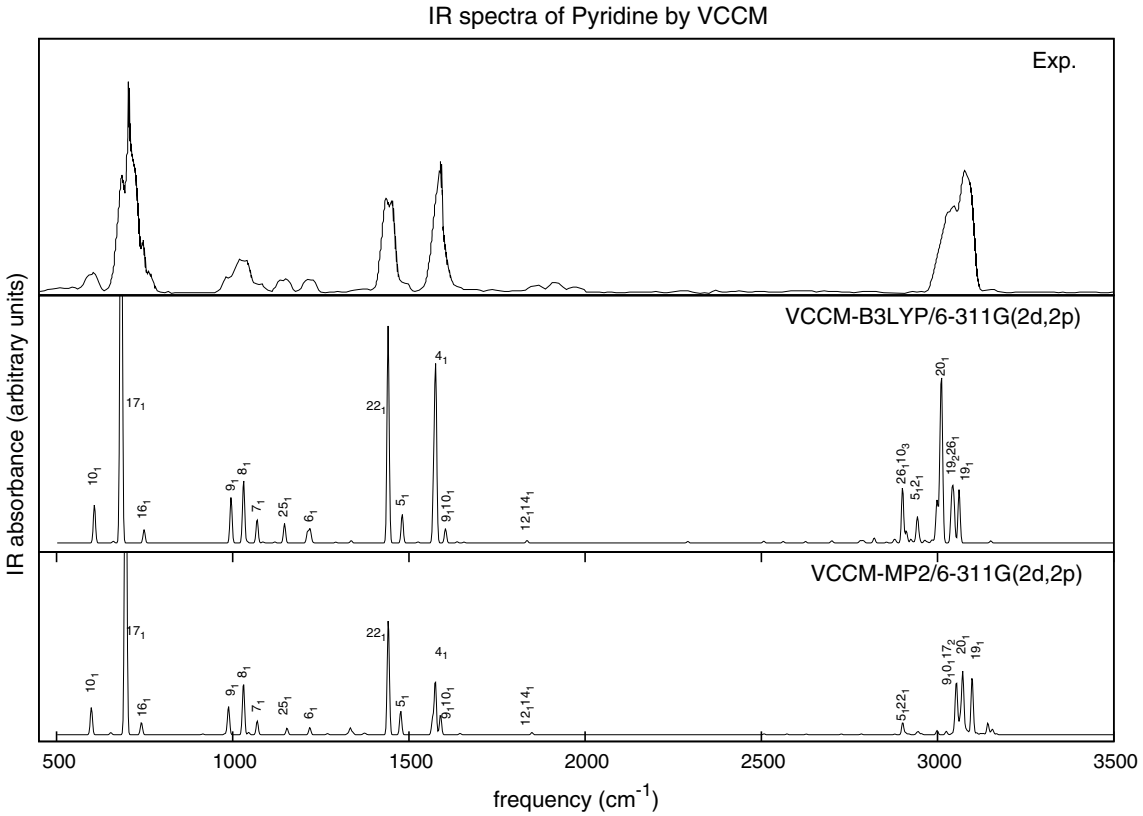

Fig. 3 Comparison of theoretical spectra of pyridine molecule calculated by VCCM method with experimental gas phase spectrum [49]

peaks. Koon and Colson [60] reported three strong transitions and one low intense transition in their experimental study. However, the B3LYP calculations give some more peaks in this regions. With MP2 calculations, we get three sharp peaks here. The vibrational resonances and near resonances are prominent in this region of spectrum. Thus, only linear terms in the DMS is not adequate for the spectral description in the region. The calculated spectra in the frequency range between 500–1700 cm^{-1} are in good agreements with the experimental one. Around frequency range 1800 cm^{-1} we found deviations between the calculated and experimental spectra. The experimental spectrum has three weak bands around frequency 1800 cm^{-1}. Our calculations shows only one very weak transition corresponds to $12_1 14_1$ at 1850 cm^{-1} with MP2-based surfaces and at 1835 cm^{-1} B3LYP with surfaces. All these three bands are due to excitations to the overtone and combination states. In inability of our calculations to produce all the three peaks and their assignments is due to the absence of the higher terms in the DMS. In between the MP2 and B3LYP, we find that both the methods give nearly identical spectrum for the region 500–2000 cm^{-1} in terms of the positions of the reported transitions.

4 Conclusions

We used two correlation methods MP2 and B3LYP and two basis sets aug-cc-pVTZ and 6-311G(2*d*,2*p*) to generate the quartic PES and linear DMS. The analysis of the standard deviations of the transition energies to the fundamental states with respect to the experimental values, we find that the MP2-based PES gives better results than the B3LYP for F_2CO molecule. For the other two molecules studied here, the differences in the standard deviations by these two methods are marginal, especially with VCCM-based calculations. Note that the PES generation with MP2 method takes longer time than the B3LYP method with a given basis set. Among two different kind of basis sets used here, we find that the Pople type 6-311G(2*d*,2*p*) basis set gives better result than the Dunning-type aug-cc-pVTZ basis set. Again, the use of 6-311G(2*d*,2*p*) basis set is computationally cheaper than aug-cc-pVTZ basis set. The deviations in the transitions energies by these two methods and basis sets do not affect the spectral assignment and their interpretation especially in the frequency range 500–2500 cm^{-1}. Thus considering the computational cost and accuracy, the B3LYP/6-311G(2*d*,2*p*) PES is most suitable among all the PES studied here.

On the other hand, the spectral intensities are greatly affected by the difference in the electronic structure calculations for the PES and DMS. Between MP2 and B3LYP methods, B3LYP gives more accurate results for the intensities of fundamental transitions for pyridine and 1,1-$F_2C_2H_2$ molecules in the VCCM calculations. For, the F_2CO molecule, the MP2 results better accuracy in the fundamental intensities than the B3LYP. In between the two basis sets used here, 6-311G(2*d*,2*p*) gives more accurate intensities than the aug-cc-pVTZ basis set.

Acknowledgments I am grateful to Professor M. Durga Prasad for his valuable suggestions and critical comments on this work. Financial support from UGC under D. S. Kothari post-doctoral fellowship scheme is acknowledged. I thank the referees for their inclusive comments to improve the paper.

References

1. Carney DG, Sprandel LL, Kern CW (1978) Adv Chem Phys 37:305
2. Bowman J (1986) Acc Chem Res 19:202
3. Bowman JM (1978) J Chem Phys 68:608
4. Christoffel KM, Bowman JM (1982) Chem Phys Lett 105:220
5. Chaban GM, Jung JO, Gerber RB (1999) J Chem Phys 111:1823
6. Jung JO, Gerber RB (1996) J Chem Phys 105:10332
7. Gerber RB, Chaban GM, Brauer B, Miller Y (2005) In: Dykstra CE, Frenking G, Kim K, Suceria G (eds) Theory and applications of computational chemistry: the first forty years, chapter 9. Elsevier, Tokyo, pp 165–194
8. Pele L, Brauer B, Gerber RB (2007) Theor Chem Acc 117:69
9. Benoit DM (2006) J Chem Phys 125:244110
10. Keceli M, Hirata S, Yagi K (2010) J Chem Phys 133:034110
11. Matsunaga N, Chaban GM, Gerber RB (2002) J Chem Phys 117:3541
12. Sibert EL (1988) J Chem Phys 88:4378
13. McCoy AB, Sibert EL (1991) J Chem Phys 95:3476
14. Iung C, Ribeiro F, Sibert EL (2006) J Phys Chem A 110:5420
15. Rauhut G (2007) J Chem Phys 127:184109
16. Heislbetz S, Rauhut G (2010) J Chem Phys 132:124102
17. Carter S, Handy NC (1986) Comput. Phys Rep 5:117
18. Barone V, Bloino J, Guido CA, Lipparini F (2010) Chem Phys Lett 496:157
19. Nagalakshmi V, Lakshminarayana V, Sumithra G, Durga Prasad M (1994) Chem Phys Lett 217:279
20. Prasad MD (2000) Indian J Chem 39A:196
21. Banik S, Pal S, Prasad MD (2008) J Chem Phys 129:134111
22. Banik S, Pal S, Prasad MD (2010) J Chem Theory Comput 6:3198
23. Banik S, Pal S, Prasad MD (2012) J Chem Phys 137:114108
24. Banik S, Prasad MD (2012) Theor Chem Acc 131:1383
25. Christiansen O (2004) J Chem Phys 120:2149
26. Seidler P, Christiansen O (2007) J Chem Phys 126:204101
27. Yagi K, Hirata S, Hirao K (2008) Phys Chem Chem Phys 10:1781
28. Christiansen O (2007) Phys Chem Chem Phys 9:2942
29. Hirata S, Hermes MR (2014) J Chem Phys 141:184111
30. Pfeiffer F, Rauhut G (2014) J Chem Phys 140:64110
31. Neff M, Rauhut G (2009) J Chem Phys 131:124129
32. Pfeiffer F, Rauhut G, Feller D, Peterson KA (2013) J Chem Phys 138:044331
33. Hansen MB, Seidler P, Gyrffy W, Christiansen O (2010) J Chem Phys 133:114102
34. Barone V (2005) J Chem Phys 122:014108

35. Hansen MB, Christiansen O, Toffoli D, Kongsted J (2008) J Chem Phys 128:174106
36. Rauhut G (2004) J Chem Phys 121:9313
37. Carbonniere P, Lucca T, Pouchan C, Rega N, Barone V (2005) J Comput Chem 26:384
38. Barone V (2004) J Chem Phys 120:3059
39. Woon DE, Dunning TH Jr (1993) J Chem Phys 98:1358
40. Frisch MJ, Pople JA, Binkley JS (1984) J Chem Phys 80:3265
41. Frisch MJ, Trucks GW, Schlegel HB, Scuseria GE, Robb MA, Cheeseman JR, Scalmani G, Barone V, Mennucci B, Petersson GA, Nakatsuji H, Caricato M, Li X, Hratchian HP, Izmaylov AF, Bloino J, Zheng G, Sonnenberg JL, Hada M, Ehara M, Toyota K, Fukuda R, Hasegawa J, Ishida M, Nakajima T, Honda Y, Kitao O, Nakai H, Vreven T, Montgomery JA Jr, Peralta JE, Ogliaro F, Bearpark M, Heyd JJ, Brothers E, Kudin KN, Staroverov VN, Kobayashi R, Normand J, Raghavachari K, Rendell A, Burant JC, Iyengar SS, Tomasi J, Cossi M, Rega N, Millam JM, Klene M, Knox JE, Cross JB, Bakken V, Adamo C, Jaramillo J, Gomperts R, Stratmann RE, Yazyev O, Austin AJ, Cammi R, Pomelli C, Ochterski JW, Martin RL, Morokuma K, Zakrzewski VG, Voth GA, Salvador P, Dannenberg JJ, Dapprich S, Daniels AD, Farkas o, Foresman JB, Ortiz JV, Cioslowski J, Fox DJ (2009) Gaussian09 Revision B.01. Gaussian Inc., Wallingford
42. Arponen J (1983) Ann Phys (NY) 151:311
43. Arponen J, Bishop RF, Pajanne E (1987) Phys Rev A 36:2519
44. Arponen J, Bishop RF, Pajanne E (1897) Phys Rev A 36:2539
45. Sastry GM, Prasad MD (1993) Theor Chim Acta 89:193
46. Latha GS, Prasad MD (1993) Theor Chim Acta 86:511
47. Prasad MD (1994) Theor Chim Acta 88:383
48. Silva AF, Soares DX, Faria SH, Bruns RE (2012) J Mol Struct 1009:49
49. Stein SE, NIST chemistry webbook, NIST standard reference database number 69, national institute of standards and technology. http://webbook.nist.gov/chemistry/
50. Smith AL (1982) In: Craver CD (ed) The Coblentz Society desk book of infrared spectra, 2nd edn. Coblentz Society, Kirkwood
51. Kagel RO, Powell DL, Overend J, Ramos MN, Bassi ABMS, Bruns RE (1982) J Chem Phys 77:1099
52. Duncan JL, Nivellini GD, Tullini F, Fusina L (1990) Chem Phys Lett 165:362
53. Wiberg KB, Walters VA, Wong KN, Colson SD (1984) J Phys Chem 88:6067
54. Walters VA, Snavely DL, Colson SD, Wiberg KB, Wong KN (1986) J Phys Chem 90:592
55. De Lorenzi A, Giorgianni S, Gambi A, Visinoni R, Stoppa P, Ghersetti S (1992) J Mol Spectrosc 151:322
56. Smith DC, Neilsen JR, Claaseen HR (1950) J Chem Phys 18:326
57. McKean DC, Veken BVD, Herrebout W, Law MM, Brenner MJ, Nemchick DJ, Craig NC (2010) J Phys Chem A 114:5728
58. Krasnoshchekov SV, Craig NC, Stepanov NF (2013) J Phys Chem A 117:3041
59. Nielsen JR, Claassen HH, Smith DC (1950) J Chem Phys 18:812
60. Wong KN, Colson SD (1984) J Mol Spectrosc 104:129
61. Partal F, Fernández-Gómez M, López-González JJ, Navarro A, Kearley GJ (2000) Chem Phys 261:239
62. DiLella DP, Stidham HD (1980) J Raman Spectrosc 9:90
63. Wiberg KB, Walters VA, Colson SD (1984) J Phys Chem 88:6067
64. Walters VA, Snavely DA, Colson SD, Wong KN (1986) J Chem Phys 90:592
65. Klots T (1998) Spectrochim Acta Part A 54:1481
66. Boese AD, Martin JML (2004) J Phys Chem A 108:3085
67. Barone V (2004) J Phys Chem A 108:4146